Forum for Electromagnetic Research Methods and Application Technologies (FERMAT)

Recent Developments in Transformation Optics-aided CEM

Ozlem Ozgun [1] and Mustafa Kuzuoglu [2]
[1] Dept. of Electrical and Electronics Eng., TED University, Ankara, Turkey
[2] Dept. of Electrical and Electronics Eng., Middle East Technical University, Ankara,Turkey
(Email: ozgunozlem@gmail.com, kuzuoglu@metu.edu.tr)

***Abstract*—This review paper presents a hybrid point of view that combines computational electromagnetics (CEM) and transformation electromagnetics/optics (TEM). The main purpose is to employ the salutary features of TEM to increase the effectiveness of finite methods (such as finite element method or finite difference methods) for solving electromagnetic boundary value problems. Synergies arising from the marriage of CEM and TEM enable us to overcome some of the difficulties, such as challenging meshing issues and high levels of computational burden, associated with the finite methods. Our previous studies basically concentrated on three types of problems: (i) modeling large-scale or multi-scale electromagnetic scattering problems; (ii) modeling curved geometries that do not conform to a Cartesian grid especially in finite difference methods; and (iii) modeling stochastic electromagnetic problems having significant uncertainty. The underlying idea is to insert transformation media into computational domain in order to alleviate certain difficulties associated with some of the meshing requirements dictated by the problem geometry. Our strategy is to create a virtual "equivalent" problem, which mimics the original problem, and which enables us to develop efficient and simple-to-use computer-aided simulation tools to solve it. This paper reviews some of our previously-published approaches based on the above strategy, and includes a discussion of some of the related issues.**

***Index Terms*—Transformation electromagnetics/optics, computational electromagnetics, anisotropic metamaterials, transformation medium, coordinate transformation, finite element method (FEM), finite difference time domain method (FDTD), Monte Carlo, multi-scale, stochastic, rough surface scattering.**

I. INTRODUCTION

Computational Electromagnetics (CEM) is an interdisciplinary area which combines applied mathematics, physics and computational science, and which has become an inevitable part of high performance engineering analysis and design. Although the importance of CEM might not be evident to the general public, it has transformed our lives during the last fifty years because almost every electrical device or system in use today is analyzed, designed or tested through the use of CEM simulation tools. Basically, the CEM involves the process of modeling the interaction of electromagnetic fields with physical objects and environment through approximations to Maxwell's equations. Although Maxwell's equations are the starting points for predicting electromagnetic phenomena, their analytical solutions are available only for a few simple canonical geometries. The invention of computers in 1940s and the fast advances thereafter in computer technology triggered the development of various computational techniques to solve Maxwell's equations for more general real-world geometries. Today there are many CEM tools that have been developed for the simulation of complex problems.

In spite of great progress achieved in the past, CEM is an evolving research area and there are still challenges that require elegant and sophisticated approaches [1] for meeting them. One of the major issues associated with the CEM techniques is the demand for intensive computational resources, such as computation time and memory, or mesh refinement to improve accuracy, when dealing with certain class of problems. For example, in multi-scale problems where a significant volume of empty space or large number of unknowns must be used to model geometries including both electrically large and small features in a medium, traditional computational techniques require resources beyond what is available today. In addition, mesh refinements or subgridding to handle fine features or curved boundaries often require special treatments which, in turn, place heavy burden on the available computational resources. Another example of CEM challenge is encountered in Monte Carlo simulation of stochastic problems, such as the one associated with rough surface scattering, which requires repeated solutions of the problem for a set of random parameters, and which demands a very heavy computational cost. This has led the CEM researchers of today to develop powerful techniques which leverage the existing numerical methods and embellish them in a way that makes it possible for them to handle complex problems that are highly computer-intensive.

Above-mentioned challenges have long been the primary concerns of researches working in the CEM field. The approach for reshaping objects by using anisotropic metamaterials in 2007 [2]-[3], which the present authors developed just after the invisibility cloaking concept was introduced in 2006 [4]-[5], inspired us to use the principles of transformation electromagnetics (TEM) to alleviate certain difficulties that arise in CEM methods. TEM provides

an intuitive and systematic way to design application-oriented transformation media (or metamaterials) to adjust the behavior of electromagnetic waves in a desired manner. It employs the principle of form-invariance of Maxwell's equations under coordinate transformations. When the spatial domain of a medium is modified by employing a coordinate transformation, this medium equivalently turns into an anisotropic medium in which Maxwell's equations retain the same mathematical form. The constitutive parameters of the anisotropic medium are determined from the Jacobian of the coordinate transformation. To put it another way, a type of duality is achieved between the modified coordinate system of the problem and the material parameters of the associated medium. Here, the most crucial issue is how the coordinate transformation is defined to create a simpler equivalent problem that mimics the field behavior of the intended original problem. Once the coordinate transformation has been defined, the relevant material parameters can be computed by following a straightforward procedure.

Although the invisibility cloaking device led to the concept of transformation electromagnetics/optics in the present form, this concept was originally introduced by Bateman at the very beginning of the 20th century [6]. One well-known application of this approach is the design of perfectly matched layer (PML), which is an artificial medium used for mesh truncation in finite methods. The approach is known as coordinate stretching in PML nomenclature, and is indeed an application of TEM with complex mapping functions [7]-[11]. Especially, the locally-conformal method in [10]-[11] proposes the use of a complex form of coordinate transformation, which easily conforms to arbitrarily-shaped curved geometries. In addition, the TEM concept has been examined in some studies within the context of finite methods in the past [12]-[14]. However, the invisibility cloak, which is perhaps the most intriguing optical device, initiated the widespread use of TEM for the systematic design of various optical and electromagnetic structures. Just after the rebirth of TEM in the context of the invisibility cloaking approach, we proposed the reshaping approach through real mapping functions, which transforms the geometry of an object into a new one of different shape [4]-[5]. Almost concurrently, Teixeira also proposed an approach for reshaping of objects in [15]. These papers in [4]-[5] and [15] are indeed the first studies extending the concept of cloaking to the design of reshaped objects to control their electromagnetic responses. Following the above, various other applications of TEM have also been proposed in the literature [16]-[41]. In spite of widespread use of TEM, it is not uncommon to run into situations where the resulting TEM-designed device is difficult to realize in practice because of difficulty in acquiring real or artificial materials that exhibit the spatial variations specified by the TEM algorithm. However, some promising realizations of such materials have been proposed in [42]-[45], and future developments in material technology may help us further in our attempt to address this problem. At this point, it is worthwhile to note that our objective in this paper is to improve CEM techniques, and the physical realization of metamaterials is beyond the scope of this work. This was also the reason why we named such materials as *software metamaterials* in one of our previous works [38].

The principal concept which underlies all of the approaches presented in this paper is to modify the computational domain, and to place suitable transformation media inside the modified domain to devise simple and efficient computer-aided simulation tools. Three types of problems are considered: (i) modeling large-scale or multi-scale electromagnetic scattering problems [35], [36], [38] (Section III); (ii) modeling curved geometries that do not conform to a Cartesian grid especially in finite difference methods [37] (Section IV); and, (iii) modeling stochastic electromagnetic problems having significant uncertainty [39]-[41] (Section V). In each section below, the corresponding problem is explained in detail and illustrative numerical examples are included.

It is useful to note that the design of the transformation medium depends on the nature of the problem. Therefore, this paper aims to provide both the basic principles and intuitive understanding of how to incorporate transformation media into CEM techniques. Although the way of defining the coordinate transformation might differ from problem to problem, the computation of the material parameters follows the same procedure and is based on the form-invariance property of Maxwell's equations. Hence, we first present the framework of transformation electromagnetics under a general coordinate transformation in Section II. Finally, some discussions and questions pertaining to the presented approach are included in Section VI.

Throughout the paper, the suppressed time dependence of the form $\exp(j\omega t)$ is assumed.

II. Overview of Transformation Electromagnetics

In this section, the general procedure of determining the material parameters of the transformation medium is explained. A general coordinate transformation, $\mathbf{r} \rightarrow \tilde{\mathbf{r}} = \mathrm{T}(\mathbf{r})$, transforms or moves each point P in the original space Ω to another point $\tilde{\mathrm{P}}$ in the transformed space $\tilde{\Omega}$. Here, $\mathbf{r}$ and $\tilde{\mathbf{r}}$ are the position vectors of the points P and $\tilde{\mathrm{P}}$ in the original and transformed coordinate systems, respectively. The transformation converts the original medium to an anisotropic medium whose constitutive parameters are obtained via the Jacobian of the transformation. The transformed fields satisfy the original form of Maxwell's equations in the anisotropic medium; hence this behavior is also known as the form-invariance property of Maxwell's equations.

If the original medium before the transformation is an isotropic medium with parameters (ε, μ), then the permittivity and permeability tensors of the anisotropic transformation medium can be expressed as [46]

$$\overline{\overline{\varepsilon}} = \varepsilon \overline{\overline{\Lambda}}, \qquad \overline{\overline{\mu}} = \mu \overline{\overline{\Lambda}}, \tag{1}$$

where

$$\overline{\overline{\Lambda}} = \delta_{\overline{\overline{\mathrm{J}}}} (\overline{\overline{\mathrm{J}}}^{\mathrm{T}} \cdot \overline{\overline{\mathrm{J}}})^{-1}, \tag{2}$$

where $\delta_{\overline{\overline{\mathrm{J}}}}$ denotes the determinant of the Jacobian tensor that is defined in Cartesian coordinates as follows:

$$\bar{\bar{\mathrm{J}}} = \frac{\partial(\tilde{x},\tilde{y},\tilde{z})}{\partial(x,y,z)} = \begin{bmatrix} \partial_x\tilde{x} & \partial_y\tilde{x} & \partial_z\tilde{x} \\ \partial_x\tilde{y} & \partial_y\tilde{y} & \partial_z\tilde{y} \\ \partial_x\tilde{z} & \partial_y\tilde{z} & \partial_z\tilde{z} \end{bmatrix}. \tag{3}$$

where $\partial_x \triangleq \partial/\partial x$, $\partial_y \triangleq \partial/\partial y$ and $\partial_z \triangleq \partial/\partial z$.

If we consider the case of electromagnetic scattering from cylindrical objects, and assume that the wave propagation is invariant along the infinite z-axis (i.e., no z-variation), then the z-dependent off-diagonal terms of (3) become zero (i.e., $\partial_z\tilde{x} = \partial_z\tilde{y} = \partial_x\tilde{z} = \partial_y\tilde{z} = 0$), as well as the z-dependent diagonal term becomes unity $\partial_z\tilde{z} = 1$. When the original medium is an anisotropic medium with parameters $(\bar{\bar{\varepsilon}}', \bar{\bar{\mu}}')$, then the parameters are computed by using

$$\bar{\bar{\varepsilon}} = \delta_{\bar{\bar{\mathrm{J}}}} \left(\bar{\bar{\mathrm{J}}}^{-1}\right)^{\mathrm{T}} \cdot \bar{\bar{\varepsilon}}' \cdot \left(\bar{\bar{\mathrm{J}}}^{-1}\right), \tag{4}$$

$$\bar{\bar{\mu}} = \delta_{\bar{\bar{\mathrm{J}}}} \left(\bar{\bar{\mathrm{J}}}^{-1}\right)^{\mathrm{T}} \cdot \bar{\bar{\mu}}' \cdot \left(\bar{\bar{\mathrm{J}}}^{-1}\right). \tag{5}$$

The Jacobian tensor can be determined either analytically or numerically. In the analytical approach, analytical functions that describe the points within the medium are defined. Consider the general form of coordinate transformation in the following:

$$\tilde{x} = f(x,y), \qquad \tilde{y} = g(x,y), \qquad \tilde{z} = z, \tag{6}$$

where f and g are functions defining the coordinate transformation. The tensor $\bar{\bar{\Lambda}}$ in (2) is computed by

$$\bar{\bar{\Lambda}} = \begin{bmatrix} \Lambda_{11} & \Lambda_{12} & 0 \\ \Lambda_{21} & \Lambda_{22} & 0 \\ 0 & 0 & \Lambda_{33} \end{bmatrix} = \left[\begin{array}{cc|c} & & 0 \\ & \bar{\bar{\Lambda}}_{\mathrm{t}} & 0 \\ \hline 0 & 0 & \Lambda_{33} \end{array}\right], \tag{7}$$

where

$$\Lambda_{11} = \frac{\delta_{\bar{\bar{\mathrm{J}}}}}{\delta_{\bar{\bar{\mathrm{J}}}^{\mathrm{T}}\cdot\bar{\bar{\mathrm{J}}}}}\left[J_{22}^2 + J_{12}^2\right], \tag{8}$$

$$\Lambda_{12} = \Lambda_{21} = -\frac{\delta_{\bar{\bar{\mathrm{J}}}}}{\delta_{\bar{\bar{\mathrm{J}}}^{\mathrm{T}}\cdot\bar{\bar{\mathrm{J}}}}}\left[J_{11}J_{12} + J_{21}J_{22}\right], \tag{9}$$

$$\Lambda_{22} = \frac{\delta_{\bar{\bar{\mathrm{J}}}}}{\delta_{\bar{\bar{\mathrm{J}}}^{\mathrm{T}}\cdot\bar{\bar{\mathrm{J}}}}}\left[J_{11}^2 + J_{21}^2\right], \tag{10}$$

$$\Lambda_{33} = \delta_{\bar{\bar{\mathrm{J}}}}. \tag{11}$$

$\delta_{\bar{\bar{\mathrm{J}}}^{\mathrm{T}}\cdot\bar{\bar{\mathrm{J}}}}$ is the determinant of $\bar{\bar{\mathrm{J}}}^{\mathrm{T}} \cdot \bar{\bar{\mathrm{J}}}$, and J_{ij} refers to the ij-th component of the Jacobian tensor.

In the numerical approach for finite element method (FEM), the points are found by using simple search techniques, and then, the Jacobian tensor is numerically computed by employing scalar basis functions. Advantages of the numerical implementation are twofold: It can be used for arbitrarily-shaped geometries and it can easily be incorporated into FEM. For example, if the computational domain is discretized by triangular elements with three nodes, each element is mapped to a master element in local coordinates (ξ,η). Based on isoparametric mapping, the coordinate variations in both original and transformed domain are obtained as follows:

$$x = \sum_{i=1}^{3} x_i N_i(\xi,\eta) \quad , \quad y = \sum_{i=1}^{3} y_i N_i(\xi,\eta), \tag{12}$$

$$\tilde{x} = \sum_{i=1}^{3} \tilde{x}_i N_i(\xi,\eta), \qquad \tilde{y} = \sum_{i=1}^{3} \tilde{y}_i N_i(\xi,\eta), \tag{13}$$

where $(x_{\mathrm{i}}, y_{\mathrm{i}})$ and $(\tilde{x}_{\mathrm{i}}, \tilde{y}_{\mathrm{i}})$ are the original and transformed nodal coordinates in each element, respectively. Here, $\mathrm{N}_{\mathrm{i}}(\xi,\eta)$ is the scalar basis function for the i-th node in local coordinates and is given by

$$N_1 = 1 - \xi - \eta, \qquad N_2 = \xi, \qquad N_3 = \eta. \tag{14}$$

By using the chain rule, the entries of the Jacobian tensor are expressed as follows:

$$\begin{bmatrix} J_{11} \\ J_{12} \end{bmatrix} = \begin{bmatrix} \partial_x\tilde{x} \\ \partial_y\tilde{x} \end{bmatrix} = \begin{bmatrix} x_2 - x_1 & y_2 - y_1 \\ x_3 - x_1 & y_3 - y_1 \end{bmatrix}^{-1} \cdot \begin{bmatrix} \tilde{x}_2 - \tilde{x}_1 \\ \tilde{x}_3 - \tilde{x}_1 \end{bmatrix}, \tag{15}$$

$$\begin{bmatrix} J_{21} \\ J_{22} \end{bmatrix} = \begin{bmatrix} \partial_x\tilde{y} \\ \partial_y\tilde{y} \end{bmatrix} = \begin{bmatrix} x_2 - x_1 & y_2 - y_1 \\ x_3 - x_1 & y_3 - y_1 \end{bmatrix}^{-1} \cdot \begin{bmatrix} \tilde{y}_2 - \tilde{y}_1 \\ \tilde{y}_3 - \tilde{y}_1 \end{bmatrix}, \tag{16}$$

which depend on the nodal coordinates that are both x- and y-dependent.

In order to show the form invariance property of Maxwell's equations, let us express the fields in a source-free medium with constitutive parameters (ε, μ) as follows:

$$\tilde{\nabla} \times \mathbf{E}(\tilde{\mathbf{r}}) = -j\omega\mu\mathbf{H}(\tilde{\mathbf{r}}), \tag{17a}$$

$$\tilde{\nabla} \times \mathbf{H}(\tilde{\mathbf{r}}) = j\omega\varepsilon\mathbf{E}(\tilde{\mathbf{r}}), \tag{17b}$$

where $\mathbf{E}(\tilde{\mathbf{r}})$ and $\mathbf{H}(\tilde{\mathbf{r}})$ are the transformed fields (i.e., mapped versions of $\mathbf{E}(\mathbf{r})$ and $\mathbf{H}(\mathbf{r})$ to the transformed space, respectively), and $\tilde{\nabla} = [\bar{\bar{\mathrm{J}}}^{-1}]^{\mathrm{T}} \cdot \nabla$ is the del operator in transformed space. Maxwell's equations in (17) are equivalent to those in the original coordinates, and they satisfy:

$$\nabla \times \tilde{\mathbf{E}}(\mathbf{r}) = -j\omega\bar{\bar{\mu}} \cdot \tilde{\mathbf{H}}(\mathbf{r}), \tag{18a}$$

$$\nabla \times \tilde{\mathbf{H}}(\mathbf{r}) = j\omega\bar{\bar{\varepsilon}} \cdot \tilde{\mathbf{E}}(\mathbf{r}). \tag{18b}$$

The fields within the transformed space are also transformed as follows:

$$\tilde{\mathbf{E}}(\mathbf{r}) = \bar{\bar{\mathrm{J}}}^{\mathrm{T}} \cdot \mathbf{E}(\tilde{\mathbf{r}}), \tag{19a}$$

$$\tilde{\mathbf{H}}(\mathbf{r}) = \bar{\bar{\mathrm{J}}}^{\mathrm{T}} \cdot \mathbf{H}(\tilde{\mathbf{r}}). \tag{19b}$$

Eqn. (19) illustrates the principle of field equivalence. The original fields in transformed coordinates [i.e., $\mathbf{E}(\tilde{\mathbf{r}})$] and the transformed fields in the original coordinates [i.e., $\tilde{\mathbf{E}}(\mathbf{r})$] are inter-related, and hence, that the original desired fields can be recovered from the fields within the transformation medium. For TM_z (transverse magnetic) case where $\mathbf{E}(\mathbf{r}) = \hat{a}_z E_z(x,y)$, (19a) reduces to $E_z(\tilde{x},\tilde{y}) = \tilde{E}_z(x,y)$.

By manipulating Maxwell's equations, the electric field satisfies the following vector wave equation in transformed and original coordinates, respectively, as follows:

$$\tilde{\nabla}\times\tilde{\nabla}\times\mathbf{E}\left(\tilde{\mathbf{r}}\right)-k^2\mathbf{E}\left(\tilde{\mathbf{r}}\right)=0\,, \tag{20}$$

$$\nabla\times\left\{\overline{\overline{\Lambda}}^{-1}\cdot\nabla\times\tilde{\mathbf{E}}\left(\mathbf{r}\right)\right\}-k^2\overline{\overline{\Lambda}}\cdot\tilde{\mathbf{E}}\left(\mathbf{r}\right)=0\,, \tag{21}$$

where k is the wave number of the original medium. For TM_z case, the vector wave equations reduce to scalar Helmholtz equations in transformed and original coordinates, respectively, as follows:

$$\tilde{\nabla}^2E_z+k^2E_z=0\,, \tag{22}$$

$$\nabla\cdot\left(\overline{\overline{\Lambda}}_{\mathrm{t}}\nabla\tilde{E}_z\right)+k^2\delta_t\Lambda_{33}\tilde{E}_z=0\,, \tag{23}$$

where δ_t is the determinant of $\overline{\overline{\Lambda}}_{\mathrm{t}}$. Within the transformation medium, (23) can be solved by using the tensors, or (22) can be solved without tensors by just replacing the coordinates with the transformed coordinates.

III. Modeling Large-Scale or Multi-Scale Electromagnetic Scattering Problems

Efficient and accurate simulations of electromagnetic boundary value problems that have multi-scale features is still a challenging problem. Multi-scale electromagnetics involves electrically large and small structures that are simultaneously present in a medium where a significant volume of empty space or mesh refinement must be used. For example, the following applications are of multi-scale nature: small antennas mounted on large platforms; feed regions of the antennas; fine-featured interconnect structures in integrated circuits, and sensors transplanted within the human body. Such problems may heavily burden the available computational resources, because they may require a large number of unknowns to model them accurately if traditional computational techniques are employed.

Application 1: Within the context of TEM, we first proposed the domain compression approach in [35]. The main goal is to design a transformation medium to compress the excessive white space in such a way that electromagnetic waves are guided inside the medium without changing the wave behavior in the rest of the domain. This technique can be used in a certain class of problems, especially having an electrically-large non-convex object or multiple objects positioned arbitrarily in space. In such problems, *excessive* white-space (i.e., free-space) must be used inside the computational domain, which introduces a large number of unknowns. This is due to the fact that the computational domain must necessarily be convex to properly account for the mutual couplings among different parts of the geometry. For example, to model an L-shaped object, a rectangular domain should be used, or the computational domain should be defined with respect to the convex hull [i.e., the smallest convex set that encloses the object(s)]. Hence, the computational domain must include excessive free-space covering the inner part of the convex hull. Another reason of why the computational domain must be convex is that absorbers (such as perfectly matched layer PML) truncating the computational domain must be designed over a convex domain in order to annihilate the outgoing waves.

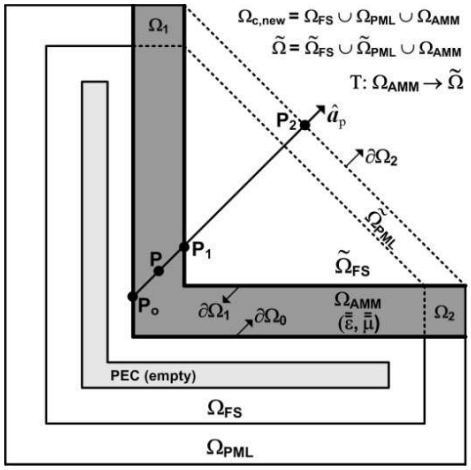

Fig. 1. Domain compression approach for L-shaped object. (Reprinted from [35], Copyright 2013, with permission from Elsevier)

Consequently, the convexity property of the computational domain is mandatory in finite methods and this, in turn, often introduces a large number of unnecessary unknowns in the free-space region. The proposed technique compresses such white space by using a transformation medium, which eliminates the unknowns in this white space and thus results in a reduction of the total number of unknowns.

Without loss of generality, the domain compression technique is shown in Fig. 1, where an L-shaped object is illuminated by a plane-wave. The original computational domain (i.e., $\Omega_{c,\,org}=\Omega_{FS}\cup\Omega_{PML}\cup\tilde{\Omega}_{FS}\cup\tilde{\Omega}_{PML}\cup\Omega_{AMM}$, where the subscripts 'FS' and 'PML' denote 'free space' and 'perfectly matched layer', respectively) is trapezoidal in shape, considering the convex-hull of the object, to minimize the number of unknowns as much as possible. The computational domain may also be of rectangular shape to be able to use certain numerical schemes based on Cartesian grids. In the proposed approach, the transformation medium layer or anisotropic metamaterial medium (Ω_{AMM}) is constructed in such a way that the excessive white space region is compressed. Computational domain of the equivalent problem becomes $\Omega_{c,\,new}=\Omega_{FS}\cup\Omega_{PML}\cup\Omega_{AMM}$ as shown in Fig. 1. In this configuration, there may be a small free-space gap between the object and the boundary of the layer ($\partial\Omega_0$).

The transformation layer is designed by mapping each point P inside the layer to $\tilde{P}$ inside the transformed region $\tilde{\Omega}=\tilde{\Omega}_{FS}\cup\tilde{\Omega}_{PML}\cup\Omega_{AMM}$. This mapping is defined as a coordinate transformation $T:\Omega_{AMM}\rightarrow\tilde{\Omega}$ as follows:

$$\tilde{\mathbf{r}}=\frac{\left\|\tilde{\mathbf{r}}_2-\tilde{\mathbf{r}}_0\right\|}{\left\|\tilde{\mathbf{r}}_1-\tilde{\mathbf{r}}_0\right\|}\left(\mathbf{r}-\tilde{\mathbf{r}}_0\right)+\tilde{\mathbf{r}}_0 \tag{24}$$

where $\mathbf{r}=(x,y,z)$ and $\tilde{\mathbf{r}}=(\tilde{x},\tilde{y},\tilde{z})$ are the position vectors of the points P and $\tilde{P}$ in the original and transformed coordinate systems, respectively, and $\|\cdot\|$ represents the Euclidean norm. Moreover, $\tilde{\mathbf{r}}_0$, $\tilde{\mathbf{r}}_1$ and $\tilde{\mathbf{r}}_2$ are the position vectors of P_0, P_1 and P_2 which are determined on $\partial\Omega_0$, $\partial\Omega_1$

and $\partial\Omega_2$, respectively, through the unit vector $\hat{\boldsymbol{a}}_p$. Through this coordinate transformation, the region $\tilde{\Omega}$ is compressed into the layer Ω_{AMM} in the direction of the unit vector $\hat{\boldsymbol{a}}_p$. The direction of the unit vector $\hat{\boldsymbol{a}}_p$ can be chosen in the direction of the parallel lines and/or in the direction of lines intersecting at a pre-defined point outside the compressed domain. In principle, the unit vector should be chosen in such a way that the domain is compressed in a symmetrical manner as much as possible. This is needed to avoid non-uniform compression (i.e., non-uniform density of transformed points) inside the layer, and thus, to avoid large variances in the entries of the constitutive tensors.

In this configuration, the PML region should also be compressed into a region inside the layer. This is necessary to avoid artificial reflections from the outer boundary $\partial\Omega_1$. The PML action can be included by using the locally-conformal PML method [10]-[11], which utilizes a special type of complex coordinate stretching. The locally-conformal PML is designed in complex space by just replacing the real coordinates with their complex counterparts (i.e., simply by adding suitable imaginary parts to the real coordinates). In this way, complex-valued permittivity and permeability tensors ($\overline{\overline{\varepsilon}}_{\text{PML}}, \overline{\overline{\mu}}_{\text{PML}}$) are obtained inside the PML layer, and the constitutive parameters of the transformation medium whose transformed points fall into the PML region are determined by (4) and (5). In other words, the principles of transformation electromagnetics are applied twice, in a consecutive manner.

The problem in Fig. 1 has been simulated by using the FEM, and the results are presented in Fig. 2. A plane wave is incident on a thin L-shaped object, whose thickness is $\lambda/20$ and edge-length is 8λ, where λ = 1m is the free-space wavelength, and the angle of incidence is 45° with respect to the *x*-axis. The element size is set to $\lambda/20$. The thickness of the transformation layer is 1λ. Fig. 2(b) shows the implementation of the coordinate transformation, carried out by using unit vectors directed along parallel lines with an angle of 45°. The computation times for the equivalent and original problems are 42 sec and 215 sec, respectively. To measure the performance of the proposed method, the mean square percentage difference is defined as $\text{Err} = \sum_{\Omega_{\text{FS}}} \left|E^{\text{e}} - E^{\text{o}}\right|^2 \Big/ \sum_{\Omega_{\text{FS}}} \left|E^{\text{o}}\right|^2$, where E^{e} and E^{o} are the electric fields calculated in the equivalent and original problems, respectively. In addition, the reduction in the number of unknowns is measured by using the following expression: $\text{N}_{\text{reduce}} = (\text{N}^{\text{o}} - \text{N}^{\text{e}})/\text{N}^{\text{o}}$, where N^{e} and N^{o} are the number of unknowns employed in the equivalent and original problems, respectively. In Table I, we tabulate the error values by varying the thickness of the transformation layer (d_{AMM}), and the element size (Δh) used in FEM. We also tabulate the N_{reduce} values in this table. We conclude that the proposed method is fast and reliable even with the moderate element sizes, and provides a considerable reduction in the number of unknowns, especially at high frequencies.

TABLE I
ERROR VALUES AND REDUCTION IN UNKNOWNS FOR L-SHAPED OBJECT (REPRINTED FROM [35], COPYRIGHT 2013, WITH PERMISSION FROM ELSEVIER)

	ERR (%)		
d_{AMM} (λ)	$\Delta\text{h} = \lambda/20$	$\Delta\text{h} = \lambda/40$	N_{reduce} (%)
0.5	0.0713	0.0306	62
0.4	0.0988	0.0942	65
0.3	0.1700	0.1310	68

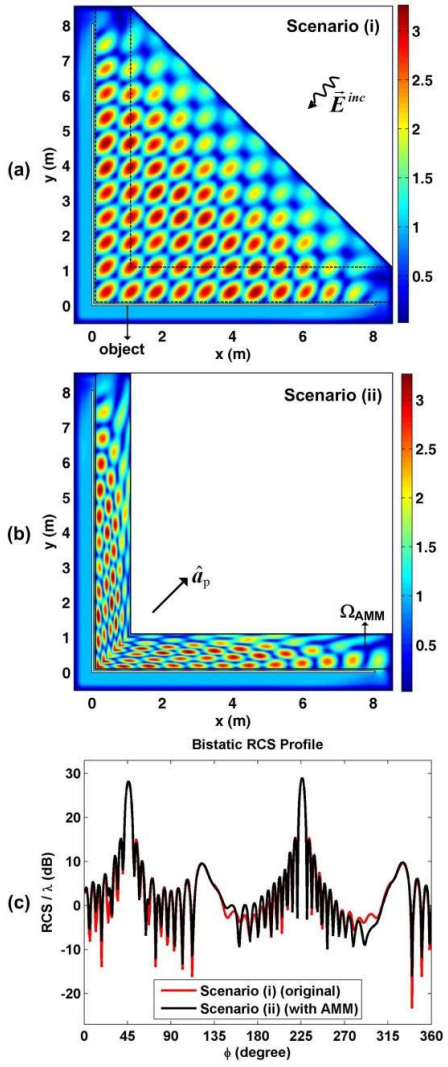

Fig. 2. Finite element simulation for L-shaped object: (a) Electric field map in original problem; (b) electric field map in equivalent problem with transformation medium; (c) bistatic radar cross-section (RCS) profile. (Reprinted from [35], Copyright 2013, with permission from Elsevier)

Application 2: Next we turn to various approaches for devising simple and efficient computer-aided simulation schemes, for multi-scale problems [36], [38]. While solving such problems with conventional finite methods, the mesh must be refined around objects with electrically-small features, in order to be able to accurately capture the field variations in their vicinity if larger-scale or coarser discretizations are employed. Hence, the main bottleneck in multi-scale problems is the high local density of number of

unknowns in modeling small-scale details within electrically large domains. The main advantage of the proposed approach is to eliminate the need for mesh refinement around the small-scale features, enabling one to employ a uniform and easy-to-generate mesh throughout.

We next consider the scattering problem involving six electrically-small circular objects, as shown in Fig. 3. Fig. 3(a) shows the standard mesh with refinement around the objects, assuming that the objects are perfectly conducting, though they can be dielectric. Fig. 3(b) shows an equivalent problem designed by inserting the transformation medium (Ω_M) around each object. The shape of the transformation medium is arbitrary, as long as its shape is convex. It may either be conformal to the object or may be adapted to the rectangular mesh as shown in this figure. The region occupied between the boundary of the object and the inner boundary of the layer is discarded. In designing the layer, each point P inside Ω_M is mapped to $\tilde{P}$ inside the transformed region $\tilde{\Omega} = \Omega \cup \Omega_M$, by using the following coordinate transformation $T : \Omega_M \to \tilde{\Omega}$

$$\mathbf{r} \to \tilde{\mathbf{r}} = T(\mathbf{r}) = \frac{\|\mathbf{r}_a - \mathbf{r}_c\|}{\|\mathbf{r}_a - \mathbf{r}_b\|}(\mathbf{r} - \mathbf{r}_b) + \mathbf{r}_c \qquad (25)$$

where $\mathbf{r}_a$, $\mathbf{r}_b$ and $\mathbf{r}_c$ are the position vectors of the points P_a, P_b and P_c, through the unit vector $\hat{\mathbf{a}}$ originating from a point inside the innermost domain (such as the center-of-mass point) in the direction of the point P within the layer. Note that if the object is perfectly conducting, Ω does not include the inner part of the object. This technique can also be extended to dielectric objects in a similar manner. In this case, $\mathbf{r}_c$ is set to zero and Ω includes the inner region. When the transformed point falls inside the dielectric object, the material parameters are computed with respect to the dielectric constant of the object. Also note that the transformation ensures that the transformed and the original coordinates are continuous along the outer boundary of the transformation medium (i.e., if $\mathbf{r} = \mathbf{r}_a$, then $\mathbf{r} = \tilde{\mathbf{r}} = \mathbf{r}_a$ on $\partial\Omega_M$).

An equivalent problem, which has a uniform mesh and fewer unknowns, is created by using the proposed transformation without resorting to mesh refinement around the object. The term "equivalence" here means that the fields within the free-space region—but outside the transformation media—are identical in both the original and equivalent problems, and that the fields inside the layer are related to the original near-fields in the vicinity of the object due to the principle of field equivalence expressed in (19). The coordinate transformation basically confines the fields around the object to the transformation medium. In other words, the transformation medium creates a virtual reality in the sense that it forces the fields inside the layer to mimic the fields within $\tilde{\Omega}$. In this manner, the boundary of the small object is moved to the inner boundary of the layer. Thus, the boundary condition which must be imposed on the boundary of the conducting object, e.g., tangential component of the total field must be zero on the boundary, must be enforced on the inner boundary of the layer in the equivalent problem. It

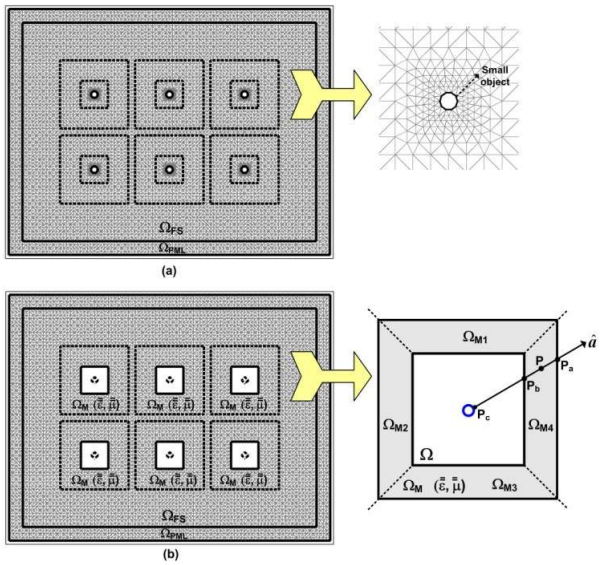

Fig. 3. Scattering from six electrically-small circular objects: (a) Original problem with refined mesh; (b) equivalent problem with separate transformation media and uniform mesh. (Reprinted from [38], Copyright 2013, with permission from Elsevier)

is also interesting to note that the *same* mesh can be used in the equivalent problem for an object of arbitrary shape by simply changing the constitutive parameters of the layer according to the geometry of the object.

The simulation results of the problem, derived via the FEM, are illustrated in Fig. 4. A plane wave is incident from an angle of 45° with respect to the *x*-axis. The radius of each circular object is λ/20 (λ = 1 m). The element size in the equivalent problem is approximately λ/40, whereas the element size in the original problem is gradually decreased around the object. Computational analysis of the simulations is tabulated in Table II. The results show good agreement, demonstrating the validity of the proposed approach. Small error value might be due to numerical approximations in FEM modeling, and spatial variations in the FEM mesh due to transformed coordinates.

Application 3: Another multi-scale problem involves an object which is coated with an electrically thin dielectric layer. In the conventional approach, the mesh inside the dielectric layer must be refined for good numerical precision if the thickness of the layer is thin. In the proposed approach, illustrated in Fig. 5, an imaginary or hypothetical region is designed in the inner part of the object. Assuming that the object is conducting, the transformation medium is the union of the imaginary and dielectric regions. The white inner region surrounded by the imaginary region is discarded from the mesh, and a uniform mesh is created within the transformation medium. The transformation medium is designed by mapping each point P inside $\Omega_M = \Omega \cup \Omega_d$ to $\tilde{P}$ inside the transformed region $\tilde{\Omega} = \Omega_d$, by using the same coordinate transformation as in (25). Note that although the same expression is used, the original and transformed domains differ in each technique. This transformation *expands* the fields within the thin layer to the transformation

TABLE II
COMPUTATIONAL ANALYSIS OF THE PROBLEM IN FIGS. 3-4. (REPRINTED FROM [38], COPYRIGHT 2013, WITH PERMISSION FROM ELSEVIER)

	Original Problem	Equivalent Problem
Time for mesh generation phase (sec)	88	76
Time for FEM matrix formation and solution phases (sec)	594	455
Total time (sec)	688	531
Matrix size	27887	25391
Matrix condition number	5.1×10^4	7.4×10^4
Mean square percentage difference (Err)	0.1951 %	

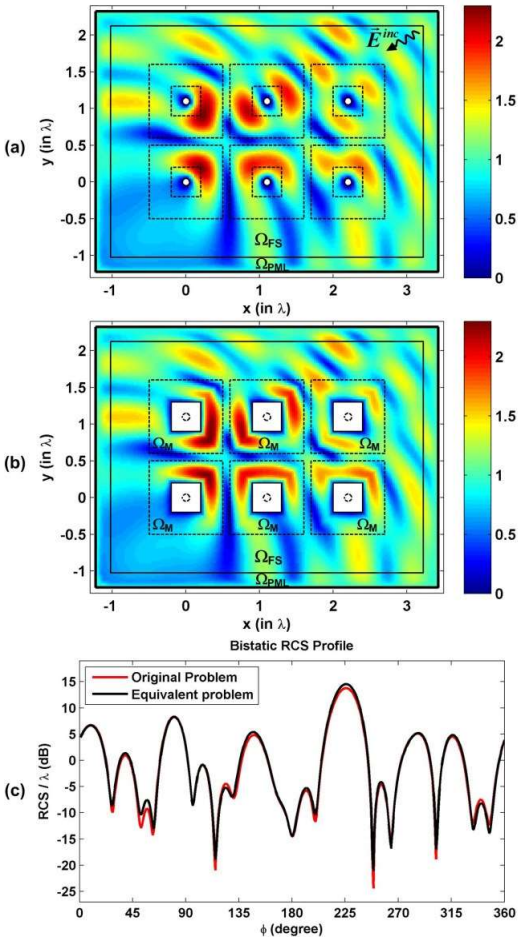

Fig. 4. Finite element simulation of scattering from six electrically-small circular objects: (a) Electric field map in original problem; (b) electric field map in equivalent problem with transformation media; (c) bistatic RCS profile. (Reprinted from [38], Copyright 2013, with permission from Elsevier)

medium. The action of the transformation medium is the field expansion, *not* the field confinement or compression. In this approach, the transformed point always lies inside the dielectric region, and hence, the parameters of the transformation medium are obtained accordingly. Common to the previous approaches, different problems (such as multiple layers with different thicknesses and dielectric constants) can be simulated by employing a single mesh, and by changing only the material parameters.

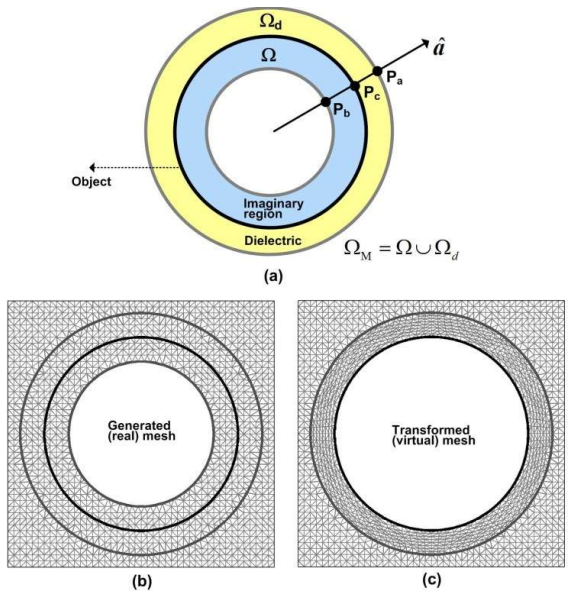

Fig. 5. Scattering from an object coated by a dielectric layer: (a) Proposed approach; (b) real physical mesh used in the simulation; (c) virtual mesh after the transformation. (Reprinted from [38], Copyright 2013, with permission from Elsevier)

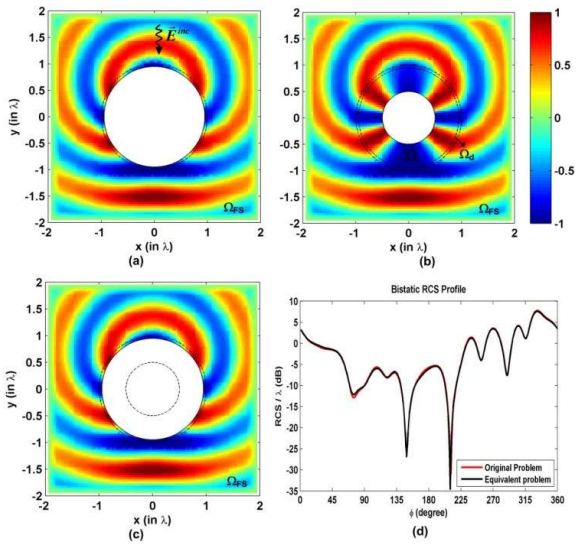

Fig. 6. Finite element simulation of scattering from a circular object coated by a dielectric layer: (a) Electric field map in original problem; (b) electric field map in equivalent problem; (c) electric field map in equivalent problem after transforming the field values by using the field equivalence; (d) RCS profiles. (In the field maps, thicknesses of the dielectric and transformation layers are λ/20 and 0.5λ, respectively. In the RCS profile, they are λ/200 and 0.1λ, respectively.) (Reprinted from [38], Copyright 2013, with permission from Elsevier)

The results of numerical simulations of the problem under consideration are presented in Fig. 6. The diameter of the circular object is 2λ. Note that Fig. 6(c) shows the field map that is plotted after transforming the field values by using the field equivalence in (19), which is the same as the field map in Fig. 6(a). This shows that desired field values in the

original problem can be recovered from the field distribution within the transformation medium of the equivalent problem.

Alternatively, thin dielectric coatings can be handled by using an approach similar to the one employed in Application 2 above. In this approach, the transformation medium can be designed outside of the object, and when the transformed point falls inside the dielectric layer, material parameters can be derived accordingly. In addition to the above applications, similar techniques can be designed, for example, for objects having electrically thin or sharp features, or objects separated by electrically-short distances. The readers are referred to [36] and [38] for further details on these alternate approaches.

IV. Elimination of Staircase Approximation of Curved Geometries in Cartesian Grids

Finite difference methods belong to the class of grid-based numerical modeling methods, and the finite difference time domain (FDTD) method is a widely-used technique, which uses a leap-frog scheme for marching on time where the electric and magnetic fields are staggered on a Cartesian coordinate grid. One of the main drawbacks of this method is the difficulty encountered when modeling curved geometries that do not conform to a Cartesian grid. It is common to utilize a staircase approximation of the curved surface, but an accurate solution can only be obtained by using very fine grids, and consequently very small time step. This obviously increases the computational load. There are some techniques reported in the literature, such as locally-conformal FDTD or use of nonorthogonal grids, to overcome this difficulty. In [37], we proposed a staircase-free approach by employing the principles of transformation electromagnetics. The main idea is to place a transformation medium that is adapted to the Cartesian grid and around the curved boundary of the object; and to discard the region between the curved boundary and the inner boundary of the transformation medium. The material parameters of the transform medium are obtained by using a coordinate transformation that maps the region inside the layer to the region between the curved boundary and the outer boundary of the layer. In this manner, curved boundaries can be modeled with simple Cartesian grids and without staircase errors.

Let us consider the geometry in Fig. 7. The upper slanted part of the object is not conformal to the Cartesian grid, and its staircase approximation causes errors because the conventional FDTD cannot well capture the field variations across this boundary. In the proposed approach, an equivalent problem is designed by placing a transformation medium (shaded by the yellow color) around the curved boundary. The region occupied between the object's boundary and the inner boundary of the layer is removed. Each point P inside Ω_A is mapped to $\tilde{P}$ inside the transformed region $\tilde{\Omega} = \Omega \cup \Omega_A$, by using the following coordinate transformation $T : \Omega_A \to \tilde{\Omega}$

$$\mathbf{r} \to \tilde{\mathbf{r}} = T(\mathbf{r}) = \frac{\|\mathbf{r}_b - \mathbf{r}_c\|}{\|\mathbf{r}_b - \mathbf{r}_a\|}(\mathbf{r} - \mathbf{r}_a) + \mathbf{r}_c \ . \qquad (26)$$

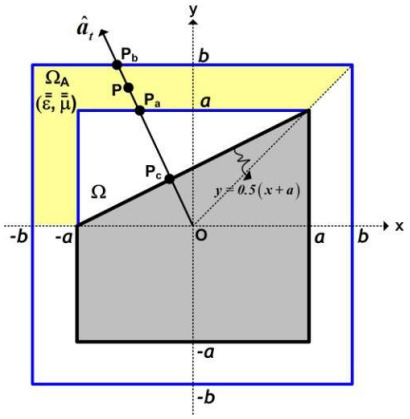

Fig. 7. Coordinate transformation technique for staircase-free FDTD method.

Note that, due to the nature of the transformation, coordinates are transformed only in the yellow region of the transformation medium. In other regions (shaded by white) surrounding the object, the transformation yields original coordinates (i.e., if $\mathbf{r}_a = \mathbf{r}_c$, then $\mathbf{r} = \tilde{\mathbf{r}}$, $\forall \mathbf{r} \in \Omega_A$). In addition, the coordinates are continuous along the outer boundary of the transformation medium (i.e., if $\mathbf{r} = \mathbf{r}_b$, then $\mathbf{r} = \tilde{\mathbf{r}} = \mathbf{r}_b$ on $\partial\Omega_A$). These conditions are indeed necessary to satisfy the field continuity.

It is worthwhile to mention that since we are concerned with the time domain method in this section, the field expressions in Sec. II are expressed in terms of both space and time. In addition, the implementation of the FDTD equations in an anisotropic medium requires a special treatment, and the readers are referred to [37] for details.

To compare the performances of the FDTD implementations in the equivalent and original problem geometries, several numerical experiments are performed. The geometry in Fig. 7 is simulated and the field maps at different time instants are presented in Fig. 8. The excitation is driven with a sine wave at 3 GHz. The original problem is staircased on a "fine" Cartesian grid to reduce the error to a certain value by adjusting the grid size sufficiently small (grid size is $\lambda/40$). In the equivalent problem, the edge lengths of the inner and outer layers of the transformation medium are set to 1λ and 2λ, respectively. The error values comparing the original and equivalent problems are listed in Table III.

V. Modeling Stochastic Electromagnetic Problems

Smooth surfaces do not really exist in the physical world; and hence, it is vital to analyze the extent to which electromagnetic waves are affected by surface roughness. There are three possible cases: (i) Scattering from a rough sea or ground surface without any other object or inhomogeneity; (ii) scattering from a composite problem where smooth objects are located on/above random rough sea or ground surface (i.e., perfectly smooth objects are in a random medium); and (iii) scattering from an object with a rough surface in a deterministic or random medium. Due to randomness, the analysis of such problems requires some

TABLE III
ERROR VALUES FOR THE PROBLEM IN FIGS. 7-8.

	Err
Time step n=800	4.68e-5
Time step n=1000	5.41e-4
Time step n=1200	7.92e-4

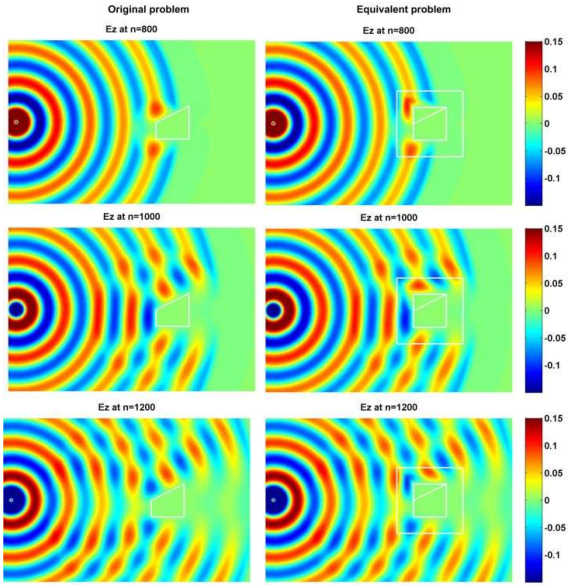

Fig. 8. FDTD field maps of original and equivalent problems at different time instants for the geometry in Fig. 7.

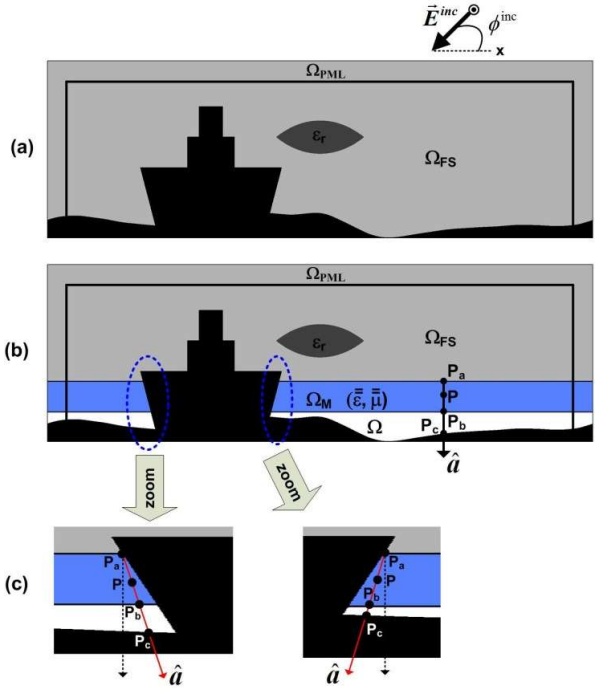

Fig. 9: Rough surface scattering problem: (a) Original scattering problem; (b) equivalent scattering problem with transformation medium; (c) part (b) in close proximity of the ship. [Ω_M : transformation medium, Ω_{FS} : free-space, Ω_{PML} : perfectly matched layer, Ω : discarded region] (Reprinted from [39], Copyright 2013, with permission from IEEE)

statistical or stochastic techniques. Monte Carlo is a commonly used technique that is utilized to generate a set of random rough surfaces from a given probability distribution, and then repeatedly solving the problem corresponding to each surface. The results are collected and formed as a random process (or random field since the domain of the underlying parameter is space rather than time). The random field is analyzed to determine the average behavior of the problem (such as mean, variance, etc). One challenging issue while realizing the Monte Carlo method is large amount of computational resources required to perform the repeated solutions for each surface. For example, if a finite method (such as finite element method or finite difference method) is to be used to solve the problem, the mesh is generated anew for each surface and the problem is solved afterwards. Eventually, the computation time increases dramatically especially in electrically large problems.

In [39], we applied the principles of transformation electromagnetics to efficiently solve the rough-surface scattering problems in cases (i) and (ii) above. The main steps of the proposed approach are as follows: (i) a single and uniform mesh is generated for the surface assuming that it is smooth; (ii) the transformation medium is placed on the smooth surface; and (iii) the material parameters of the medium are computed by using the Jacobian of a specially-defined coordinate transformation that maps the points within the transformation medium to the actual space around the rough surface. In this manner, a "virtual" equivalent problem working with a smooth surface and an anisotropic medium is created, which mimics the behavior of the original problem working with the rough surface. Therefore, a type of illusion is created to simplify the Monte Carlo analysis. Each time the surface changes, only the material parameters are modified without changing the mesh.

Similar approaches were utilized for the analysis of irregularities in waveguides having rough surfaces or grooves on the surfaces in [40], and ridges in [41]. In this paper, only the scattering problem from rough sea surfaces in [39] is discussed. The readers are referred to [40] and [41] for waveguide problems.

Without loss of generality, the technique is demonstrated by considering the geometry in Fig. 9 involving objects on or above the surface, illuminated by a plane wave. In the proposed technique in Fig. 9(b), an equivalent problem is designed by placing a transformation medium (Ω_M) above the surface. The region occupied between the boundary of the rough surface and the inner boundary of the transformation medium is discarded. Each point P inside Ω_M is mapped to $\tilde{P}$ inside the transformed region $\tilde{\Omega} = \Omega \cup \Omega_M$, by using the following coordinate transformation $T : \Omega_M \to \tilde{\Omega}$

$$\mathbf{r} \to \tilde{\mathbf{r}} = T(\mathbf{r}) = \frac{\|\mathbf{r}_a - \mathbf{r}_c\|}{\|\mathbf{r}_a - \mathbf{r}_b\|}(\mathbf{r} - \mathbf{r}_b) + \mathbf{r}_c \tag{27}$$

The unit vector is chosen to be orthogonal to the surface for each point within the transformation medium from the ship (i.e., $\hat{\mathbf{a}} = -\hat{\mathbf{a}}_y$ if vertical axis is chosen to be the *y*-axis), but it is tilted and emanating from the corner point P_a for each point in close proximity of the ship (see Fig. 9(c)). Note

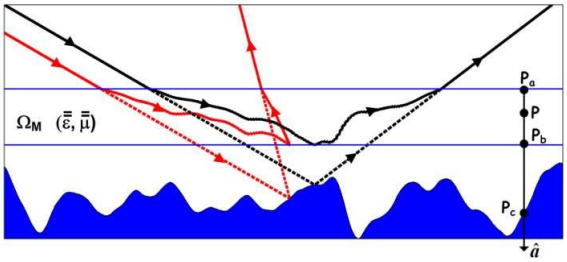

Fig. 10. Ray optics interpretation of the field behavior in the original and equivalent problems. (Dashed and solid rays correspond to original and equivalent problems, respectively.)

that, in regions other than those shown Fig. 9(c), the transformation reduces to the following simple form because of the special form of the unit vector, as follows:

$$\tilde{x} = x\,, \qquad \tilde{y} = K\left(y - y_b\right) + y_c\,, \qquad \tilde{z} = z\,, \tag{28}$$

where $K = \left|y_a - y_c\right| / \left|y_a - y_b\right|$ and $d_m = \left|y_a - y_b\right|$ is the thickness of the transformation medium. Here, y_a, y_b and y_c are the y-coordinates of the corresponding points.

The main objective of the coordinate transformation is to confine the fields to the transformation medium. To better understand the field behavior within the transformation medium, ray optics is used as shown in Fig. 10 for an arbitrarily rough surface. The dashed and solid curves show the rays in the original problem and the equivalent problem with the transformation medium, respectively. In the equivalent problem, the transformation forces the fields inside the transformation medium to imitate the fields within the region between the rough surface and the uppermost boundary of the medium. The fields outside the transformation medium are identical in both original and equivalent problems.

The performance of the proposed technique is validated through some numerical simulations. Two types of analyses are performed:

(i) Solution of a *deterministic* problem—without randomness—for a single surface realization,

(ii) Solution of a *stochastic* problem by Monte Carlo simulations. Monte Carlo method determines the average behavior of a stochastic system by repeated sampling. It is based on following main steps: (i) a set of inputs (a set of surfaces in our case) is randomly generated from a given probability distribution; (ii) deterministic computations (repeated solutions via proposed approach in our case) are performed for each input; and (iii) the results (RCS, field or error in our case) are aggregated to statistically characterize the problem on the average sense. The data generated from repeated computations can be represented as approximate probability distributions (or histograms), or some statistical parameters (such as mean, variance, etc.).

In the simulations below, rough surfaces are generated by using the Gaussian random process based on the Pierson-Moskowitz spectrum. The wind speed is u = 15 m/s, the element size is $\lambda/30$ (λ = 1 m), the thickness of the transformation medium is 2λ, and the dielectric constant of the ogive object is $\varepsilon_r = 3$. Electrical parameters of the sea

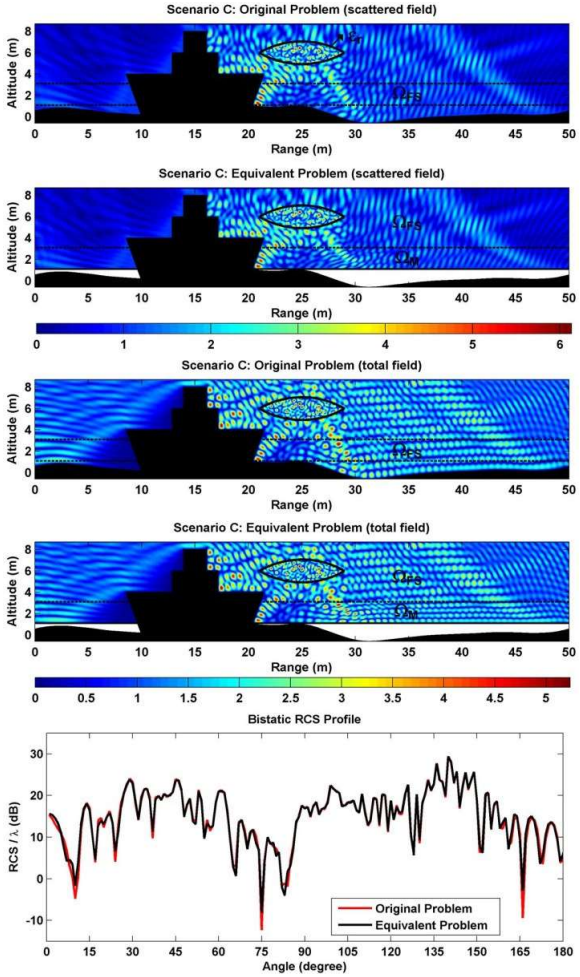

Fig. 11: Validation of the technique with comparison to the conventional FEM by considering a single surface realization: (top) Scattered and total field maps for original and equivalent problems; (bottom) bistatic RCS profiles. (Reprinted from [39], Copyright 2013, with permission from IEEE)

surface are set to $\varepsilon_r = 80$ and $\sigma = 4.8$ S/m. The computational domain is illuminated by a plane wave whose angle of incidence is $\phi^{inc} = 45°$, which is measured with respect to the x-axis in Cartesian coordinates. The plane wave is numerically tapered by the PML layer to avoid edge effects in the finite-sized domain.

First, we consider the deterministic problem assuming a single surface realization, whose results are shown in Fig. 11. The mean square percentage difference (Err) between the fields of original and equivalent problems is computed as 0.3%. Next, we perform Monte Carlo simulations by generating 100 surfaces. In this manner, a family of bistatic RCS values is obtained, for observation angles ranging from 0 to 180°, and represented as a random process. The results are shown in Fig. 12. In this figure, part (a) shows the mean RCS (sometimes called coherent component) which represents the RCS values resulting from the large scale features of the geometry because of the averaging (or smoothing) operation. Part (b) illustrates the standard deviation (STD) of the RCS values (also called incoherent

TABLE IV
COMPUTATIONAL ANALYSIS OF THE ROUGH SURFACE SCATTERING PROBLEM (REPRINTED FROM [39], COPYRIGHT 2013, WITH PERMISSION FROM IEEE)

	Original Problem	Equivalent Problem
Time for mesh generation phase (100 realizations) (min)	363	10.2 (only once)
Time for FEM matrix formation and solution phases (100 realizations) (min)	287	230
Total time (100 realizations) (min)	650	240.2
Matrix size	332,992	303,951
Matrix condition number	4.13×10^5	3.41×10^5

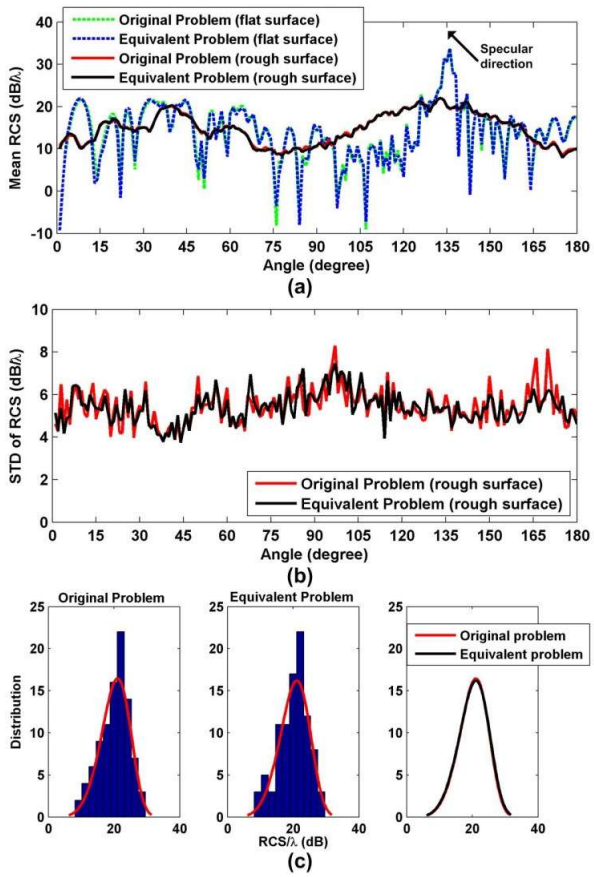

Fig. 12. [Monte Carlo] Validation of the technique with comparison to the conventional FEM by considering 100 surface realizations: (a) Ensemble mean of bistatic RCS; (b) ensemble standard deviation (STD) of bistatic RCS; (c) histograms and Weibull distributions of the RCS values at the direction of specular reflection. (Reprinted from [39], Copyright 2013, with permission from IEEE)

component), which shows the amount of variation or fluctuation in the values. Finally, part (c) plots the histograms and the Weibull probability density function of the RCS values at the specular reflection direction. Moreover, the statistical parameters of the mean square percentage difference comparing the original and equivalent problems are computed as follows: mean = 0.4%, STD = 0.2%, max = 1.0%, min = 0.1%. Finally, the computational analysis is tabulated in Table IV.

VI. DISCUSSIONS

This section aims to address some issues related to different aspects of the approaches described in the sections above. While some of these issues are addressed, other questions are left open to encourage future studies and to help generate possible discussions on this paper following its publication.

Issue 1: The transformation medium designed for an electrically-small object acts like a "magnifier". The problem involving an electrically-small object is indeed a low-frequency problem, and the transformation medium turns the low-frequency problem into a relatively high-frequency problem so that uniform mesh scheme is used. Looking at this problem from a different viewpoint, the proposed approach can be employed for radar cross-section (RCS) reduction such that a 'large' object which has a relatively large RCS values can be transformed into a 'smaller' object with reduced RCS. In other words, the transformation medium coated on the surface of an object to achieve virtual shaping can be used as an alternative to physical shaping or radar absorbing materials for RCS reduction. The overall action of the transformation medium makes sense, but *does this medium introduce an additional physical insight in terms of the wave behavior within the medium?* In fact, since the geometry is modified even in the virtual sense, the phase velocity of the electromagnetic wave should vary over a wide range to mimic the desired wave behavior of the original problem. For example, in the case where the object shrinks down to a smaller size, the wave inside the medium must travel faster along the boundary of the object in order to be in-phase at the shadow region of the object and to create the same fields in the outside medium as those of the smaller object. If this happens, then the phase velocity exceeds the velocity of light in free-space, which is the speed limit of the universe. For a non-dispersive medium, since the group velocity is equal to the phase velocity, the transformation medium must necessarily be dispersive and operate at a single frequency in order not to violate the laws of physics. This is especially important in the time domain modeling of the medium due to causality and stability issues. The transformation medium with relative permittivity and permeability values smaller than unity can operate over very narrow bandwidths, and a special treatment is needed for broadband operation. One possible solution for broader bandwidth might be to model the transformation medium as several concentric non-dispersive layers made up with *natural* material parameters having relative permittivity and permeability values *not* smaller than unity. This problem will be investigated by the authors in the future. But, in the meantime, we may pose the question: "*Without changing the material properties, is it possible to modify the stability conditions in the FDTD method to achieve a broadband medium?*"

Issue 2: Yet another important question: "*Is there any computational complexity in implementing the coordinate transformation and incorporating the anisotropic material tensors to the numerical method under consideration?*"

The computational effort in realizing the coordinate transformation in a finite element code imposes almost

negligible burden on the processing power of the computer, compared to some other phases of the code, such as usual matrix construction and solution. This is because the transformed coordinates can be determined in the preprocessing phase, i.e., before the matrix construction phase, by utilizing some simple search algorithms to find the points on the boundaries. After determining the transformed coordinates, the Jacobian tensor and the material parameters within the medium can easily be obtained by using the simple expressions in (15) and (16). In the matrix formation phase, the straightforward finite element formulation of (23) is considered in the transformation medium. In the FDTD modeling, the transformed points and the material tensors are determined, before the start of the simulation by using the analytical expressions given in (7)-(11). Although the formulation of the FDTD in an anisotropic medium (given in [37]) requires more effort in deriving the equations, it only increases the computational burden of the simulation process just slightly.

Issue 3: Next we ask a question, related to the domain compression approach: "*In the domain compression approach where a larger domain is compressed into a smaller domain, does the transformation medium require finer grid to handle field variations?*"

The principles of ray-optics enable us to conclude that the medium does *not* necessarily have to be denser. In [35], we explained this issue by considering the L-shaped geometry in Fig. 1. Let us assume that the object is illuminated by an arbitrary angle as shown in Fig. 13. In Fig. 13(a), the first- and second-order reflected rays from the lower and upper faces, respectively, are shown in the original problem. In the equivalent problem in Fig. 13(b), the domain is compressed in the direction of the unit vector which is in the same direction as that of the incident field. The first- and second-order reflected rays after the transformation are shown by $1'$ and $2'$, respectively. The length of the first ray will always be longer than its original length ($\ell_{1'} > \ell_1$) because of the compression, irrespective of the point where the incident wave hits the object. Hence, the ray must travel faster to traverse over this longer path. The wavelength increases for fixed frequency and therefore, the spatial discretization (or element size) in the original problem is sufficient. It even provides better resolution in the equivalent problem to handle field variations over this longer path. Next, let us examine the second-order reflected ray $2'$. The length of the $2'$ ray gets shorter after the transformation, and a finer discretization is required over this path due to shorter wavelength. Therefore, the only source of error will be the rough discretization over $2'$. However, since the effect and the strength of the second-order ray is less than of the first-order ray, the error levels remain acceptable. The worst case for which the length of the $2'$ ray is the shortest occurs if the direction of $2'$ is in the same direction as the unit vector denoting the direction of compression, as shown in Fig. 13(b). If the direction of the unit vector is modified as shown in Fig. 13(c), then the length of the second order ray increases ($\ell_{2''} > \ell_{2'}$), and the error due to discretization decreases. In principle, if there is wave propagation in the direction of compression, it introduces errors based on the

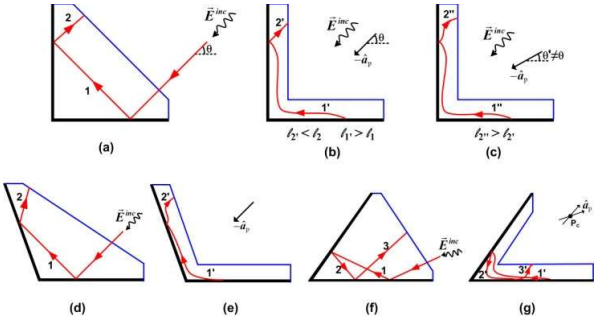

Fig. 13. Ray-optics interpretation of domain compression technique: (a) Rays in original problem of L-shaped object; (b) rays in the transformation medium if the directions of compression and propagation are the same; (c) rays in the medium if the directions of compression and propagation are different; (d) rays in original problem of wide-angle object; (e) rays in the medium of wide-angle object; (f) rays in original problem of narrow-angle object; (g) rays in the medium of narrow-angle object. (Reprinted from [35], Copyright 2013, with permission from Elsevier)

compression rate because of the decrease in the length of propagation. Otherwise, the discretization error will not occur. Hence, by adjusting the direction of compression based on the physics of the problem at hand, reliable results can be achieved and the number of unknowns can be decreased without using finer meshes. Note that due to non-convexity, the waves propagating in the direction of compression become the second- or higher-order waves, whose error contributions are small. Similar analyses are shown for a wide-angle object in Figs.13(d) and 13(e), and a narrow-angle object in Figs. 13(f) and 13(g). In Fig. 13(e), the only source of error is the second-order ray; however, the worst-case for which the compression direction is in the direction of propagation is never experienced. Similarly, in Fig. 13(g), only the third-order ray causes error. Note that the incident ray is not considered because the scattered field formulation is used. These comments are applicable to the diffracted fields as well.

Issue 4: The next question we ask is: "*Does transformation electromagnetics cause mesh deformations?*" This indeed depends on how the coordinate transformation is defined. The unit vector and the thickness of the transformation medium affect the spatial distribution of the transformed coordinates. In principle, the following condition should be kept in mind: Two closely-located points $\vec{r}$ and $\vec{r}^{\,*}$ in the medium Ω_{M} are mapped to two closely-located points $\tilde{\vec{r}}$ and $\tilde{\vec{r}}^{\,*}$ in $\tilde{\Omega}$. Mathematically, given $\varepsilon > 0$ there exists $\delta > 0$ (δ depends on ε) such that $\left\| \mathrm{T}(\vec{r}) - \mathrm{T}(\vec{r}^{\,*}) \right\| < \varepsilon$ whenever $\left\| \vec{r} - \vec{r}^{\,*} \right\| < \delta$. In other words, the deviation in relative positions for two closely-located points after the coordinate transformation should not be large. The reason is twofold: (i) spatial variations in the entries of the material parameters corresponding to contiguous points should not be large; (ii) qualities of elements in the mesh should not be distorted. Since any mesh distortion leads to an increase in the condition number, we have computed the condition numbers in our simulations and have concluded that if the coordinate transformation is defined properly by considering the continuity condition

mentioned above, the order of the condition number remains almost the same (see Tables II and IV). The mesh structure can also be visualized by plotting the virtual mesh after the transformation, similar to Fig. 5(c). Furthermore, as the thickness of the transformation medium increases, the error values tend to decrease because of the decrease in the spatial variations of the material parameters. Although the error values tend to decrease for thicker layers, we have observed in the simulations that even a thin medium layer provides reliable results.

Issue 5: Our next question is: "*What do we gain by using Transformation EM in Monte Carlo simulations?"* In Monte Carlo simulation of stochastic problems, such as rough surface scattering problems, repeated solutions are required to get a family of data for different rough surfaces. In other words, after producing a set of surface geometries, a mesh must be generated with respect to each of these geometries, and a matrix system must be formed and solved anew for each mesh. This obviously increases the computation time and memory, given the large number of realizations. The main advantage of the transformation electromagnetics is that it allows us to create a *single* mesh, which is simply constructed for a smooth surface; hence, it avoids the need for repeated mesh generations, and saves a large amount of computation time. In addition, the matrix is also generated only once, and only the part of the matrix corresponding to the transformation medium is modified during the simulations. It is useful to note that in the conventional approach, the part of the mesh above the rough surface, which does not change for different realizations, can be treated separately, and the mesh and matrix associated with this region need to be created only once. However, it should be realized that the mesh just above the surface needs to be generated for each different geometry and to be incorporated into the global mesh. Since the number of nodes and elements, as well as their numbering schemes change in each mesh generation, a computational effort is needed to combine the meshes and the matrices properly by using a unique numbering scheme at each time. Therefore, in any case, the transformation medium provides considerable advantages over the conventional approach in terms of both simplicity and computation time. Evidence of this saving may be found in Table IV.

REFERENCES

[1] R. Mittra, "A look at some challenging problems in computational electromagnetics," *IEEE Antennas and Propagation Magazine,* vol. 46, no. 5, pp. 18-32, 2004.

[2] O. Ozgun, and M. Kuzuoglu, "Electromagnetic metamorphosis: Reshaping scatterers via conformal anisotropic metamaterial coatings," *Microwave Opt. Technol. Lett*., vol. 49, no. 10, pp. 2386-2392, 2007.

[3] O. Ozgun, and M. Kuzuoglu, "Utilization of anisotropic metamaterial layers in waveguide miniaturization and transitions," *IEEE Microwave and Wireless Components Letters*, vol. 17, no. 11, pp. 754-756, 2007.

[4] J. B. Pendry, D. Schurig, D. R. Smith, "Controlling electromagnetic fields," *Science,* vol. 312, pp. 1780-1782, 2006.

[5] U. Leonhardt, "Optical Conformal Mapping", *Science*, vol. 312, pp. 1777-1780, 2006.

[6] H. Bateman, "The transformation of the electrodynamical equations," *Proc. London Math. Soc*., vol. 8, pp. 223-264, 1910.

[7] W. C. Chew, and W. Weedon, "A 3D perfectly matched medium from modified Maxwell's equations with stretched coordinates," *Microwave Opt. Technol. Lett*., vol. 7, pp. 599-604, 1994.

[8] M. Kuzuoglu, and R. Mittra, "Investigation of nonplanar perfectly matched absorbers for finite element mesh truncation," *IEEE Trans. Antennas Propagat*., vol. 45, pp. 474-486, 1997.

[9] F. L. Teixeira, and W. C. Chew, "Differential forms, metrics, and the reflectionless absorption of electromagnetic waves," *J. Electromagn. Waves Applicat*., vol. 13, pp. 665-686, 1999.

[10] O. Ozgun, and M. Kuzuoglu, "Non-Maxwellian locally-conformal PML absorbers for finite element mesh truncation," *IEEE Trans. Antennas Propagat*., vol. 55, no. 3, pp. 931-937, 2007.

[11] O. Ozgun, and M. Kuzuoglu, "Near-field Performance Analysis of Locally-conformal Perfectly Matched Absorbers via Monte Carlo Simulations," *Journal of Computational Physics*, vol. 227, no. 2, pp. 1225-1245, 2007.

[12] A. J. Ward, and J. B. Pendry, "Refraction and geometry in Maxwell's equations," *J. Mod. Opt*., vol. 43, no. 4, pp. 773-793, 1996.

[13] F. L. Teixeira, and W. C. Chew, "Lattice electromagnetic theory from a topological viewpoint," *J. Math. Phys*., vol. 40, no. 1, pp. 169-187, 1999.

[14] A. Bossavit, "On the notion of anisotropy in constitutive laws: Some implications of the 'Hodge implies metric' result," *COMPE*L, vol. 20, no. 1, pp. 233-9, 2001.

[15] F. L. Teixeira, "Closed-form metamaterial blueprints for electromagnetic masking of arbitrarily shaped convex PEC objects," *IEEE Antennas Wireless Propagat. Lett*., vol. 6, pp. 163-164, 2007.

[16] F. Kong, B.I. Wu, J.A. Kong, J. Huangfu, S. Xi, and H. Chen, "Planar focusing antenna design by using coordinate transformation technology," *Applied Physics Letters*, vol. 91, article no. 253509, 2007.

[17] B. Donderici, and F.L. Teixeira, "Metamaterial blueprints for reflectionless waveguide bends," *IEEE Microwave and Wireless Components Letters*, vol. 18, pp. 233-235, 2008.

[18] I. Gallina, G. Castaldi, and V. Galdi, "Transformation Media for Thin Planar Retrodirective Reflectors," *IEEE Antennas and Wireless Propagation Letters*, vol. 7, pp. 603-605, 2008.

[19] G.X. Yu, W.X. Jiang, X.Y. Zhou, and T.J. Cui, "Non-rotationally invariant invisibility cloaks and concentrators of EM Waves," *Eur. Phys. J. Appl. Phys*, vol. 44, pp. 181-185, 2008.

[20] D.-H. Kwon, and D. H. Werner, "Transformation optical designs for wave collimators, flat lenses, and right-angle bends," *New Journal of Physics*, no. 10, 115023, 2008.

[21] B. Vasic, G. Isic, R. Gajic and K. Hingerl, "Coordinate transformation based design of confined metamaterial structures," *Physical Review B*, vol. 79, article no. 085103, 2009.

[22] P.H. Tichit, S.N. Burokur, and A. Lustrac, "Ultradirective antenna via transformation optics," *Journal of Applied Physics*, vol. 105, article no. 104912, 2009.

[23] W. X. Jiang, J. Y. Chin, and T. J. Cui, "Anisotropic metamaterial devices," *Materials Today*, vol. 12, no. 12, pp. 26-33, 2009.

[24] F. L. Teixeira, H. Odabasi, K.F. Warnick, "Anisotropic metamaterial blueprints for cladding control of waveguide modes," *J. Opt. Soc. Am. B*, vol. 27, pp. 1603-1609, 2010.

[25] D. R. Smith, Y. Urzhumov, N. B. Kundtz, and N. I. Landy, "Enhancing imaging systems using transformation optics," *Opt. Express,* vol. 18, 21238, 2010.

[26] H. Odabasi, F. L. Teixeira, and W. C. Chew, "Impedance-matched absorbers and optical pseudo black holes," *J. Opt. Soc. Am. B*, vol. 28, no. 5, pp. 1317-1323, 2011.

[27] R. Yang, W. Tang, and Y. Hao, "A broadband zone plate lens from transformation optics," *Optics Express*, vol. 19.13, 12348-12355, 2011.

[28] K. Zhang, F. Meng, Q. Wu, J.-H. Fu, and L.-W. Li, "Waveguide connector constructed by normal layered dielectric materials based on embedded optical transformation," *European Phys. Letters*, vol. 99, 47008, 2012.

[29] M. Casaletti, C. D. Giovampaola, S. Maci, G. Vecchi, "Entire-domain basis functions for scattering from large curved surfaces formulated by transformation optics," *IEEE Trans. Antennas Propagat*., vol. 60, pp. 4271-4280, 2012.

[30] G. Castaldi, S. Savoia, V. Galdi, A. Alu, and N. Engheta, "PT Metamaterials via Complex-Coordinate Transformation Optics," *Physical Review Letter*s, vol. 110, 173901, 2013.

[31] R. Mittra, Y. Zhou, "Designing Cloaks and Absorbing Blankets for Scattering Reduction Using Field and Impedance Transformation Techniques," Chapter 14 of Computational Electromagnetics, Recent Advances and Engineering Applications (Book), Springer, 2014 ISBN 978-1-4614-4381-0, R. Mittra (Ed.).

[32] O. Ozgun, and M. Kuzuoglu, "Efficient Finite Element Solution of Low-Frequency Scattering Problems via Anisotropic Metamaterial Layers," *Microwave and Optical Technology Letters*, vol. 50, no. 3, pp. 639-646, 2008.

[33] O. Ozgun, and M. Kuzuoglu, "Form-invariance of Maxwell's Equations in Waveguide Cross-section Transformations," *Electromagnetics*, vol.29, no. 4, pp. 353-376, 2009.

[34] O. Ozgun, and M. Kuzuoglu, "Form Invariance of Maxwell's Equations: The Pathway to Novel Metamaterial Specifications for Electromagnetic Reshaping," *IEEE Antennas and Propagation Magazine*, vol. 52, no. 3, pp. 51-65, 2010.

[35] O. Ozgun, and M. Kuzuoglu, "Domain Compression via Anisotropic Metamaterials designed by Coordinate Transformations," *Journal of Computational Physics*, vol. 229, no. 3, pp. 921-932, 2010.

[36] O. Ozgun, and M. Kuzuoglu, "Numerical Solution of Multi-scale Electromagnetic Boundary Value Problems by Utilizing Transformation-based Metamaterials," *Lecture Notes in Computer Science*, volume 6785/2011, pp. 11-25, 2011.

[37] O. Ozgun, and M. Kuzuoglu, "Transformation-based Metamaterials to Eliminate the FDTD Staircasing Error", *Int. Journal of RF and Microwave Computer-Aided Engineering (Special Issue on Metamaterials: RF and Microwave Applications)*, vol. 22, no. 4, pp. 530-540, July 2012.

[38] O. Ozgun, and M. Kuzuoglu, "Software Metamaterials: Transformation Media Based Multiscale Techniques for Computational Electromagnetics," *Journal of Computational Physics*, vol. 236, pp. 203-219, March 2013.

[39] O. Ozgun, and M. Kuzuoglu, "A Transformation Media Based Approach for Efficient Monte Carlo Analysis of Scattering from Rough Surfaces with Objects," *IEEE Transactions on Antennas and Propagation*, vol. 61, no. 3, pp. 1352 - 1362, March 2013.

[40] O. Ozgun, and M. Kuzuoglu, "Transformation Electromagnetics Based Analysis of Waveguides with Random Rough or Periodic Grooved Surfaces," *IEEE Transactions on Microwave Theory and Techniques*, vol. 61, no. 2, pp. 709 - 719, Feb. 2013.

[41] O. Ozgun, and M. Kuzuoglu, "Monte Carlo Analysis of Ridged Waveguides with Transformation Media," *International Journal of RF and Microwave Computer-Aided Engineering* (*special issue on Modeling and Simulation Challenges in Microwave Engineering*), vol. 23, no. 4, pp. 476 – 481, July 2013.

[42] D. Schurig, J. J. Mock, B. J. Justice, S. A. Cummer, J. B. Pendry, A. F. Starr, and D. R. Smith, "Metamaterial electromagnetic cloak at microwave frequencies," *Science*, vol. 314, pp. 977-980, 2006.

[43] B. Edwards, A. Alu, M. G. Silveirinha, and N. Engheta, "Experimental verification of plasmonic cloaking at microwave frequencies with metamaterials," *Phys. Rev. Lett*., vol. 103, 153901, 2009.

[44] Q. Cheng, T. J. Cui, W. X. Jiang, and B. G. Cai, "An omnidirectional electromagnetic absorber made of metamaterials," *New J. Phys*., vol. 12, no. 6, 063006, 2010.

[45] X.-Y. He, C. Yang, B. Li, Q. Chen, B.-H. Zhou, and C.-X. Tang, "Experimental verification of the bending of electromagnetic waves using metamaterials," *Appl. Phys. Lett*., vol. 98, 204105, 2011.

[46] I.V. Lindell, Methods for Electromagnetic Field Analysis, Oxford Univ. Press, 1992.

Ozlem Ozgun received the Ph.D. degree in electrical engineering from Middle East Technical University (METU), Ankara, Turkey, in 2007. She was with the same university between 2008-2012. She is now an associate professor in TED University, Ankara, Turkey. Her main research interests are computational electromagnetics, finite element method, domain decomposition, electromagnetic propagation and scattering, transformation electromagnetics, and stochastic electromagnetic problems.

Mustafa Kuzuoglu received the B.Sc., M.Sc., and Ph.D. degrees in electrical engineering from the Middle East Technical University (METU), Ankara, Turkey, in 1979, 1981, and 1986, respectively. He is currently a Professor in the same university. His research interests include computational electromagnetics, inverse problems and radars.

Editorial Comment

In this paper, Ozgun and her colleague take the TO to a different direction than the conventional one, and apply it to solve Computational EM problems involving complex geometries in an interesting and non-traditional way. They show how a problem that involves a complex geometrical shape can be transformed into a simpler one, in order to gain some advantage over conventional techniques in terms of simplified mesh generation in FEM, for instance.